Diffuse Reflectance Spectroscopy of Changes in Tumor Microenvironment in Response to Different Doses of Radiation

April Jules[a], **Davin Means**[b], **Joel Rodriguez Troncoso**[a], **Alric Fernandes**[c], **Sina Dadgar**[a], **Eric R. Siegel**[d], **Narasimhan Rajaram**[a]

[a]Department of Biomedical Engineering, University of Arkansas, Fayetteville, Arkansas

[b]Department of Biological Sciences, University of Arkansas, Fayetteville, Arkansas

[c]Department of Chemistry and Biochemistry, University of Arkansas, Fayetteville, Arkansas

[d]Department of Biostatistics, University of Arkansas for Medical Sciences, Little Rock, Arkansas

Abstract

Radiation therapy plays an important role in cancer treatment, as it is an established method used as part of the treatment plan for the majority of cancer patients. Real-time monitoring of the effects of radiation on the tumor microenvironment can contribute to the development of better treatment plans. In this study, we use diffuse reflectance spectroscopy, a non-invasive optical fiber-based technique, to determine the effects of different doses of radiation on the tumor microenvironment, as well as to determine the sensitivity of diffuse reflectance spectroscopy to low doses of radiation that are used in the treatment of certain cancers. We injected 4T1 cells into 50 Balb/c mice to generate tumor xenografts. When the tumors grew to 200 mm^3, we distributed the mice into a control group or one of three radiation groups: 1, 2, or 4 Gy/fraction, and they underwent treatment for five consecutive days. We measured the tumor volume and collected diffuse reflectance spectra every day, with optical measurements being acquired both before and one h postirradiation on the five days of treatment. Based on the diffusely reflected light, we quantified vascular oxygenation, total hemoglobin content, and tissue scattering within these tumors. There was a significant increase in tumor vascular oxygenation, which was primarily due to an increase in oxygenated hemoglobin, in response to a 1 Gy/fraction of radiation, while there was a decrease in tissue scattering in response to all doses of radiation. Immunohistochemical analysis revealed that tumor cell proliferation and apoptosis were higher in irradiated groups compared to the control group. Our findings show that diffuse reflectance spectroscopy is sensitive to microenvironmental changes in tumors treated with doses of radiation as low as 1 Gy/fraction.

INTRODUCTION

Radiation therapy is currently one of the most effective components of cancer treatment, whether it is used alone or in combination with other modalities such as chemotherapy, surgery, or immunotherapy (1). The exposure of tumor cells to ionizing radiation triggers biological processes that inhibit growth and prevent cells from further proliferation. This

Address for correspondence: University of Arkansas, 700 W. Research Center Blvd., Fayetteville, AR 72701; afjules@uark.edu.

alters the metabolism of these cells and induces different forms of cell damage and death (2, 3). The delivery of treatment through fractionated radiation doses, whereby the total dose is divided into multiple fractions, has been shown to be protective of normal cells over cancer cells, as these relatively slower proliferating normal cells have more time to repair radiation-induced damage before replication (1). Fractionated regimes also promote reoxygenation of hypoxic tumor cells, resulting in increased sensitivity to subsequent fractions of radiation (4, 5). Hypoxic tumors have been shown to be more resistant to radiation (4, 5). Therefore, reoxygenation of tumor cells after irradiation increases the efficacy of the treatment (6, 7).

The tumor microenvironment (TME), which consists of blood vessels, immune cells, extracellular matrix, and various associated tissue cells, differs from the microenvironment of normal tissue, and impacts tumor progression and therefore the response of a tumor to radiation (8–11). While fibroblasts, which are a major constituent of the stroma, in normal tissue act to suppress tumor growth and progression via direct interactions with neighboring abnormal cells, cancer-associated fibroblasts in the TME promote tumorigenic activities (11). Changes in the TME due to treatment with radiation have been examined from several perspectives, including that of tumor hypoxia and changes to the tumor vasculature (8, 12–15), and superficial damage caused by these changes have been evaluated using an array of optical techniques (16). Oxygen-sensing electrodes that measure tissue oxygen partial pressure (pO$_2$) have been used to detect oxygenation in tumors prior to and during irradiation (12, 17). However, this method of evaluating treatment response is invasive, therefore limiting the measurement frequency (18, 19). Diffuse reflectance spectroscopy (DRS) is a non-invasive optical fiber-based technique that uses non-ionizing radiation to interrogate tissue. When the light interacts with components in the tissue, scattering and absorption occur, and the diffusely reflected light is collected. Analysis of the wavelength-dependent optical parameters can reveal information about relevant biological properties in the tissue (20). Several studies have used DRS to measure changes in tumor vascular oxygenation and total hemoglobin concentration in response to immunotherapy, chemotherapy, and radiation therapy (19, 21–27). Diaz et al. previously demonstrated that DRS is sensitive to radiation-induced changes in tumor oxygenation in radiation-resistant and radiation-sensitive tumors treated with 2 Gy/fraction (22). Hu et al. observed changes in oxygen and perfusion kinetics associated with doses greater than 8 Gy of fractionated radiation in mice bearing FaDu xenografts using DRS (19).

The goal of this study was to determine the sensitivity of diffuse reflectance spectroscopy to different doses of radiation on the tumor microenvironment. Specifically, we aimed to determine the changes in optical properties as a function of time and radiation dose, investigate the source of these changes in oxygenation, hemoglobin concentration and tissue scattering, and determine the relationship between reoxygenation and anatomical and functional measures of the tumor. Tumors were treated with either sham treatment, or 1, 2 or 4 Gy once a day for five days, and optical spectra were acquired before and after treatment on each day. Our results indicate that DRS can be used to detect tumor microenvironmental changes in tumors treated with low doses of radiation, as low as 1 Gy/fraction.

MATERIALS AND METHODS

Cell Culture and Tumor Xenograft Development, and Irradiation

All animal studies were approved by the Institutional Animal Care and Use Committee (IACUC) at the University of Arkansas (Protocol number: 20033). Figure 1A shows the timeline for these studies. 4T1 cells, originally derived from a spontaneous breast tumor growing in a Balb/c mouse (15) were kindly provided by Dr. Fred Miller (Karmanos Cancer Institute). Cells were cultured in Dulbecco's Modified Eagle's Medium (DMEM) with the addition of 10% fetal bovine serum (FBS), 200 mM L-glutamine, 1% nonessential amino acids, and 1% penicillin-streptomycin. The cells were cultured twice a week and stored in a humidified incubator set to 5% CO_2 and 37°C. Fifty female Balb/c mice that were 6–8 weeks old and weighing approximately 20–25 g were injected subcutaneously in the right flank with 250,000 4T1 murine mammary carcinoma cells suspended in saline. Tumor growth was monitored daily, and tumor dimensions were measured using Vernier calipers. The tumor volumes were calculated according to the equation: $V = \frac{\pi}{6} \times (width)^2 \times length$ At tumor volumes of approximately 200–250 mm^3, mice were randomly assigned to one of three treatment groups receiving either 1 Gy (n = 14), 2 Gy (n = 14) or 4 Gy (n = 12) per day, or to a control group (n = 10). Analysis of tumor optical properties was restricted to tumor data which met threshold requirements for the lookup table-based model on day 1 of measurements, and tumors from mice that survived at least five days of radiation treatment. Here, baseline refers to measurements acquired prior to the first radiation dose.

Fractionated Irradiations of Tumor Xenografts

Radiation doses of 1, 2 or 4 Gy per day were administered for 5 consecutive days. Irradiation was performed using the X-RAD 320 biological X-ray irradiator (Precision X-Ray, North Branford, CT). The mice were anesthetized using a mixture of isoflurane gas (1.5% v/v) and medical grade air through a delivery device placed within the radiation cabinet and placed on a platform 50 mm away from the X-ray source. A collimated X-ray beam was produced at a dose rate of 0.82 Gy/min, focusing exclusively on the tumor-bearing flank, with the rest of the body being shielded by lead blocks.

Diffuse Reflectance Spectroscopy

We used a DRS setup as described previously (28). The DRS system consists of a tungsten halogen lamp (HL-2000, Ocean Optics, Dunedin, FL), a USB spectrometer (Flame, Ocean Optics, Dunedin, FL), and a bifurcated fiber optic probe with source-detector separation of 2.25 mm. DRS spectra were acquired in the wavelength range of 475 to 600 nm. The common end of the probe consists of four central illumination fibers and five peripheral detector fibers. An 80% reflectance standard (SRS-80-010; Labsphere, North Sutton, NH) was used to calibrate the reflectance spectra daily to correct for potential variations in light throughput. DRS spectra were acquired twice a day on the five days of treatment, and once per day on days 6–10 after the end of radiation treatment, with about 5–10 spectra being obtained per tumor. On the treatment days, spectra were acquired prior to irradiation and 1 h postirradiation (22, 26).

Quantification of Tissue Optical Properties

We used a lookup table (LUT)-based model, constructed from the absorption coefficient and reduced scattering coefficient, to fit the measured diffuse reflectance spectra and quantify the optical properties of the tumor, specifically vascular oxygenation (sO_2), total hemoglobin concentration (THb), and tissue scattering (20, 29). The concentrations of oxygenated hemoglobin (HbO_2) and deoxygenated hemoglobin (dHb) were calculated from measured vascular oxygenation: $sO_2 = \frac{HbO_2}{THb}$ and total hemoglobin concentration: $THb = HbO_2 + dHb$. Light scattering in tissue was measured via DRS. Optical properties for each animal were determined from an average of the multiple spectra acquired, and the averages were then logarithmically transformed prior to conducting statistical analysis.

Immunohistochemistry

An intraperitoneal (i.p.) injection of 60 mg/kg pimonidazole (Hypoxyprobe, Burlington, MA) was administered to each mouse 1 h prior to euthanasia. One h post injection, tumors were resected, the mice were euthanized, and the tumors were embedded in optimal cutting temperature (OCT) compound and flash frozen using liquid nitrogen. Frozen tumors were sectioned into 10 μm slices using a cryostat (CM 1860; Leica, Inc., Nussloch, Germany), and the samples were immunostained using a direct labeling protocol. After the slides were hydrated in phosphate-buffered saline (PBS), we used a pap pen (Vector Laboratories, Burlingame, CA) to create a hydrophobic barrier around each tissue sample. The tissue sections were then fixed with 4% paraformaldehyde, permeabilized with 0.5% Triton-X 100, and incubated with a blocking solution (95% PBS, 4% goat serum, 1% sodium azide) at room temperature for 1 h. Pimonidazole staining was performed by incubating tissue sections with monoclonal antibody conjugated to Dylight™ 549 fluorophore (Hypoxyprobe Red 549 kit; HPI, Inc., Burlington, MA) for 1 h at room temperature. Ki-67 staining was done by incubating tissue sections in Ki-67 antibody (Abcam, Cambridge, MA) in a humidity chamber overnight at 4°C, followed by Alexa Fluor 647 secondary antibody (A-21244; Thermo Fisher, Waltham, MA) for 1 h at room temperature. TUNEL staining was performed as recommended by the manufacturer (In Situ Cell Death Detection Kit, Fluorescein; Roche, Mannheim, Germany). Finally, the samples were rinsed in PBS, covered with fluoromount, and slides were cover slipped with nail polish and left to dry for 24 h. The tumor sections were imaged using a confocal laser-scanning microscope (Fluoview FV10i; Olympus) and analyzed using MATLAB (Mathworks, Natick, MA).

Statistical Analysis

Statistical analyses were conducted using GraphPad Prism 9. Prior to statistical analysis, the measured data were logarithmically transformed to reduce skewness of the data. Two-way repeated measures analysis of variance (ANOVA) was used to determine statistically significant differences in tumor volume between each group over the course of the study, as well as significant differences in vascular oxygenation, total hemoglobin concentration, oxygenated hemoglobin, deoxygenated hemoglobin and scattering between time points within each treatment group. Time and radiation dose were considered fixed effects. Post-hoc analysis was conducted using Tukey's test. For all statistical analyses, P values less than 0.05 were considered significant.

RESULTS

Lower Radiation Doses Lead to a Reduction In Tumor Growth Rate

Tumor growth curves for each treatment group are shown in Fig. 1B. Our results show that on day 2 of treatment, the tumor volume in the 2 Gy group was 37.5% lower than the 4 Gy group ($P = 0.01$), and 34.4% lower than the untreated control group on day 4 ($P = 0.04$). We found that radiation, particularly at 1 Gy and 2 Gy per fraction led to a reduction in the tumor growth rate during the five days of treatment. We also compared the values of tumor volume, vascular oxygenation, total hemoglobin content and tissue scattering across all groups from measurements obtained prior to treatment on the first day. There were no significant differences in average baseline values of tumor volume (Fig. 1C) or total hemoglobin content (Fig. 1E) between the groups prior to treatment. However, the average baseline vascular oxygenation in the 2 Gy group was 62.0% higher than that of the 1 Gy group (Fig. 1D; $P = 0.03$), and the average tissue scattering was 50.1% higher in the 2 Gy group compared to the 4 Gy group. (Fig. 1F; $P = 0.009$).

Tumors Iradiated at 1 Gy Per Fraction Display Prominent Reflectance Band and Absorption Peaks

In the well-established absorption profiles of oxygenated (HbO_2) and deoxygenated hemoglobin (dHb) shown in Fig. 2A, HbO_2 has distinct dual peaks at 542 nm and 576 nm, while dHb has a single peak at 556 nm (30). Figure 2B presents in vivo DRS measurements obtained prior to treatment on day 3 from representative tumors in each treatment group and their corresponding LUT fits. Figure 2C illustrates the corresponding LUT-extracted wavelength-dependent absorption coefficients. The flatter reflectance band and single absorption peak from the non-irradiated tumor indicates lower oxygenation compared to the more pronounced reflectance band and distinct double absorption peaks displayed by the tumor irradiated at 1 Gy. The representative tumors irradiated at 2 Gy and 4 Gy also display pronounced reflectance bands and absorption peaks, although lower in magnitude and not as prominent as the tumor irradiated at 1 Gy.

Tumor Vascular Oxygenation and Oxygenated Hemoglobin Concentration Increase in Response to a Dose of 1 Gy per Fraction

We quantified the optical properties from the measured DRS spectra to determine radiation-induced changes in oxygenation. Figure 3A presents the measurements of vascular oxygenation on each day before treatment for irradiated and non-irradiated groups. Oxygenation in tumors treated with 1 Gy dose/fraction increased by 55.6%, 47.5% and 46.5% on days 3, 4, and 5, respectively, compared with the pre-irradiation baseline, yet the tumors treated with daily 4 Gy fractions the oxygenation level increased by 35.0% on day 5 relative to day 1. In the non-irradiated group, there was a 37.8% and 35.5% increase on day 5 relative to days 1 and 3, respectively. Figure 3B shows the changes in total hemoglobin for each group before irradiation on the five days of treatment. While there was an overall increase in total hemoglobin concentration in irradiated tumors, there were no significant differences within groups or among the groups. We also compared oxygenated hemoglobin (Fig. 3C) and deoxygenated hemoglobin (Fig. 3D) in each treatment group on the five days of radiation treatment. The changes in oxygenated hemoglobin were greater than that of

deoxygenated hemoglobin. This was particularly noticeable in the 1 Gy group. Statistical analysis of this data showed increases of 63.5% and 62.0% in oxygenated hemoglobin on days 4 and 5 of treatment, respectively, relative to the pre-irradiated baseline. In the 4 Gy group, oxygenated hemoglobin increased by 51.1% on day 5 compared with day 1. There was also a 15.4% reduction in deoxygenated hemoglobin in the 1 Gy group on day 5 of treatment relative to day 1.

Tumor Cell Proliferation and Apoptosis are Higher in Irradiated Groups Compared to Control Groups

We used immunohistochemistry (IHC) staining to assess sections from tumors collected after five days of radiation treatment or no treatment, shown in Fig. 4. The tumors irradiated at 2 Gy/fraction showed the highest pimonidazole expression, while those irradiated at 4 Gy/fraction expressed the lowest percentage of pixels positively stained for pimonidazole (Fig. 4A), with a statistically significant difference between the two groups (P = 0.02). Ki-67 expression was lowest in the non-irradiated tumors and was similar in irradiated tumors (Fig. 4F). Tumors irradiated at 4 Gy/fraction had the highest percentage of TUNEL-positive pixels, while non-irradiated tumors showed low levels of TUNEL (Fig. 4K).

Tissue Scattering Decreases in Response to Irradiation and is not Correlated with Cell Proliferation and Apoptosis

There was an overall decrease in tissue scattering in all groups across the five days of treatment (Fig. 5), noticeably in the 2 Gy group where scattering decreased by 30.1% on day 4 compared to day 1. However, an increase in scattering was observed in all the groups after receiving four doses of radiation, or prior to treatment on day 5. We also determined the association between optical scattering in the tumors and cell proliferation and apoptosis assessed by IHC staining (data not shown). There was a weak positive correlation between Ki-67 positive stained pixels and mean reduced scattering coefficient and a similar negative correlation between the percentage of pixels positively stained for TUNEL and mean reduced scattering coefficient; however, these correlations were not statistically significant

DISCUSSION

Previous studies examining the effects of radiation on the tumor microenvironment using optical spectroscopy have done so using a single high dose or high-dose irradiations greater than 8 Gy per fraction (19, 31). Clément-Colmou et al. recently investigated the effects of high-dose fractionated irradiations on the phenotype and functionality of the tumor vasculature (8). In this study, we measured changes in the tumor microenvironment in response to low doses of fractionated irradiations using diffuse reflectance spectroscopy. We saw changes in vascular oxygenation and total hemoglobin concentration with respect to time and radiation dose. Tumor oxygenation is one of the microenvironmental factors that affects response to radiation. Reoxygenation in tumors after fractionated irradiations has been investigated by several groups, and early reoxygenation has been attributed to a decrease in oxygen consumption and increase in oxygen supply (6, 26). Short-term changes in tumor oxygenation after irradiation have also been investigated as a marker for radiation response (22), and it has been shown previously that tumor irradiation can affect blood flow

(32–34). We found that tumor vascular oxygenation increased in all the radiation groups, but we observed a significant increase in response to a radiation dose of 1 Gy/fraction during treatment (Fig. 3A). This was also evident in the pronounced reflectance band and prominent peaks seen in the absorption spectrum of the representative 1 Gy tumor on day 3 of treatment, indicating the presence of oxygenated hemoglobin. While the baseline vascular oxygenation for some of the tumors in this group was relatively low, the baseline volumes for those tumors were within the range of baseline tumor volumes that we selected for this study, and multiple optical spectra were acquired from each tumor. Understanding changes in hemoglobin concentration is essential in examining radiation-induced changes in the tumor microenvironment, and has recently been studied using optical techniques like hyperspectral imaging (35). Using diffuse reflectance spectroscopy, we found that while there was an overall increase in total hemoglobin concentration throughout the course of treatment, it did not change significantly (Fig. 3B) but there was an increase in oxygenated hemoglobin concentration (Fig. 3C). Therefore, the primary driver of changes in vascular oxygenation are due to changes in oxygenated hemoglobin.

In addition to measuring vascular oxygenation, we used IHC techniques to validate these changes in oxygenation. Tumor hypoxia, or low-oxygen supply to tissue, is problematic for radiotherapy and affects treatment outcome. Several methods have been used to detect tumor hypoxia, including polarographic O_2 sensors, PET imaging, and IHC methods using markers like pimonidazole, a well-established method for quantifying hypoxia (36). Palmer et al. found that using optical spectroscopy to detect changes in tissue oxygenation in tumors was comparable to the established partial oxygen pressure system where the sensors were inserted into the tumors (37). Dadgar et al. showed that oxygenation measurements obtained by DRS are consistent with pimonidazole quantification in head and neck cancer xenografts, and can be used as a measure of hypoxic fraction (28). In this study, we found that while the percentage of pimonidazole positive pixels was similar among all groups, the highest percentage was seen in tumors irradiated at 2 Gy/fraction (Fig. 4A–E). This is consistent with our finding that the 2 Gy/fraction group showed the lowest levels of oxygenation after five days of treatment with radiation.

To assess tumor cell proliferation and apoptosis in response to radiation, we conducted Ki-67 and TUNEL staining, respectively. Vala et al. exposed human lung microvascular endothelial cells to doses of radiation lower than 2 Gy and found that doses lower than 1 Gy did not affect cell proliferation but above 1 Gy, the proliferation rate significantly decreased (38). We saw a contrasting trend in this study. While proliferation was lowest in non-irradiated tumors, it was similar for tumors across all radiation groups, and there was no significant difference in percentage of Ki-67 positive pixels in control tumors and irradiated tumors (Fig. 4F–J). In their study, Chung et al. observed that tissues with higher levels of oxygenation contained more proliferative cells (39). We did not make such an observation with our data, however, as the Ki-67 levels were similar among all groups. Ionizing radiation is known to induce DNA damage as well as cell death via apoptosis or necrosis (40, 41). TUNEL staining illustrated differences between the groups receiving radiation and the control group, particularly in the 4 Gy/fraction group in which the tumor sections had a higher quantity of TUNEL positive pixels (Fig. 4K–O). Radiation at higher

doses is expected to cause greater damage, rendering the cells more susceptible to cell death (42).

Light scattering in tissue can be extracted from DRS measurements by quantification of the reduced scattering coefficient, which is typically modelled as a power law, from which scattering amplitude and scattering exponent can be derived. Changes in optical scattering in tissue can be impacted by multiple factors, including alterations to morphological features of cell organelles such as mitochondria and nuclei (43), as well as changes in tumor volume which can be affected by cell proliferation and apoptosis (44). Although we did not observe any significant differences in tissue scattering between the treatment groups, we saw a decrease in scattering in all groups (Fig. 5). Tabassum et al., in treating tumors with chemotherapy and antiangiogenic agents, correlated optical parameters derived from spatial frequency domain imaging (SFDI), a wide-field technique used to quantify scattering and absorption due to chromophores in tissue, with tumor physiological markers. They found that an increase in scattering amplitude is strongly correlated with apoptosis, and a decrease in scattering exponent is strongly correlated with cell proliferation (45), however in studying these parameters in the context of radiation treatment, we did not observe such correlations. From our assessment of tumor cell proliferation and apoptosis and their relationship with tissue scattering, we saw a weak positive correlation between scattering and Ki-67 positive pixels and a weak negative correlation between scattering and TUNEL positive pixels, but neither were statistically significant. While scattering may be associated with an increase in cell proliferation as well as nuclear and mitochondrial fragmentation due to apoptosis (46), longitudinal IHC data may have been better able to determine such a relationship in our study.

In summary, diffuse reflectance spectroscopy has been used as a non-invasive technique to measure optical properties of tissue, and we have demonstrated that this method can be used to detect changes in the tumor microenvironment in response to low doses of radiation, as low as 1 Gy/fraction. We were able to detect an increase in vascular oxygenation in irradiated tumors, largely due to an increase in oxygenated hemoglobin concentration. Additional frequent, near-real-time measurements of tumor function are necessary as this provides knowledge of reoxygenation and can be used to determine the frequency with which tumors should be irradiated.

ACKNOWLEDGMENTS

REFERENCES

1. Baskar R, Lee KA, Yeo R, Yeoh KW. Cancer and radiation therapy: current advances and future directions. Int J Med Sci. 2012; 9(3):193–9. [PubMed: 22408567]

2. Wu Q, Allouch A, Martins I, Brenner C, Modjtahedi N, Deutsch E, et al. Modulating both tumor cell death and innate immunity is essential for improving radiation therapy effectiveness. Front Immunol. 2017; 8:613. [PubMed: 28603525]

3. Wang JS, Wang HJ, Qian HL. Biological effects of radiation on cancer cells. Mil Med Res. 2018; 5(1):20. [PubMed: 29958545]

4. Potiron VA, Abderrahmani R, Clément-Colmou K, Marionneau-Lambot S, Oullier T, Paris F, et al. Improved functionality of the vasculature during conventionally fractionated radiation therapy of prostate cancer. PloS One. 2013; 8(12):e84076. [PubMed: 24391887]

5. Brown JM. Tumor hypoxia in cancer therapy. Methods Enzymol. 2007; 435:295–321.

6. Crokart N, Jordan BF, Baudelet C, Ansiaux R, Sonveaux P, Grégoire V, et al. Early reoxygenation in tumors after irradiation: determining factors and consequences for radiotherapy regimens using daily multiple fractions. Int J Radiat Oncol Biol Phys. 2005; 63(3):901–10. [PubMed: 16199320]

7. Chen Z, Guo W, Wu Q, Tan L, Ma T, Fu C, et al. Tumor reoxygenation for enhanced combination of radiation therapy and microwave thermal therapy using oxygen generation in situ by CuO nanosuperparticles under microwave irradiation. Theranostics. 2020; 10(10):4659–4675. [PubMed: 32292521]

8. Clément-Colmou K, Potiron V, Pietri M, Guillonneau M, Jouglar E, Chiavassa S, et al. Influence of Radiotherapy Fractionation Schedule on the Tumor Vascular Microenvironment in Prostate and Lung Cancer Models. Cancers (Basel). 2020; 12(1):121. [PubMed: 31906502]

9. Kizaka-Kondoh S, Inoue M, Harada H, Hiraoka M. Tumor hypoxia: a target for selective cancer therapy. Cancer Sci. 2003; 94(12):1021–8. [PubMed: 14662015]

10. Hirata E, Sahai E. Tumor microenvironment and differential responses to therapy. Cold Spring Harb Perspect Med. 201; 7(7):a026781.

11. Alkasalias T, Moyano-Galceran L, Arsenian-Henriksson M, Lehti K. Fibroblasts in the tumor microenvironment: shield or spear? Int J Mol Sci. 2018; 19(5):1532. [PubMed: 29883428]

12. Nordsmark M, Bentzen SM, Rudat V, Brizel D, Lartigau E, Stadler P, et al. Prognostic value of tumor oxygenation in 397 head and neck tumors after primary radiation therapy. An international multi-center study. Radiother Oncol. 2005; 77(1):18–24. [PubMed: 16098619]

13. Paidi SK, Diaz PM, Dadgar S, Jenkins SV, Quick CM, Griffin RJ, et al. Label-free Raman spectroscopy reveals signatures of radiation resistance in the tumor microenvironment. Cancer Res. 2019; 79(8):2054–64. [PubMed: 30819665]

14. Moeller BJ, Cao Y, Li CY, Dewhirst MW. Radiation activates HIF-1 to regulate vascular radiosensitivity in tumors: role of reoxygenation, free radicals, and stress granules. Cancer Cell. 2004; 5(5):429–41. [PubMed: 15144951]

15. Garcia-Barros M, Paris F, Cordon-Cardo C, Lyden D, Rafii S, Haimovitz-Friedman A, et al. Tumor response to radiotherapy regulated by endothelial cell apoptosis. Science. 2003; 300(5622):1155–9. [PubMed: 12750523]

16. Abdlaty R, Hayward J, Farrell T, Fang Q. Skin erythema and pigmentation: a review of optical assessment techniques. Photodiagnosis Photodyn Ther. 2021; 33:102127. [PubMed: 33276114]

17. Ressel A, Weiss C, Feyerabend T. Tumor oxygenation after radiotherapy, chemotherapy, and/or hyperthermia predicts tumor free survival. Int J Radiat Oncol Biol Phys. 2001; 49(4):1119–25. [PubMed: 11240254]

18. Nordsmark M, Loncaster J, Chou S-C, Havsteen H, Lindegaard JC, Davidson SE, et al. Invasive oxygen measurements and pimonidazole labeling in human cervix carcinoma. Int J Radiat Oncol Biol Phys. 2001; 49(2):581–6. [PubMed: 11173158]

19. Hu F, Vishwanath K, Salama JK, Erkanli A, Peterson B, Oleson JR, et al. Oxygen and perfusion kinetics in response to fractionated radiation therapy in FaDu head and neck cancer xenografts are related to treatment outcome. Int J Radiat Oncol Biol Phys. 2016; 96(2):462–9. [PubMed: 27598811]

20. Nichols BS, Rajaram N, Tunnell JW. Performance of a lookup table-based approach for measuring tissue optical properties with diffuse optical spectroscopy. J Biomed Opt. 2012; 17(5):057001. [PubMed: 22612140]

21. Glennie DL, Hayward JE, McKee DE, Farrell TJ. Inexpensive diffuse reflectance spectroscopy system for measuring changes in tissue optical properties. J Biomed Opt. 2014; 19(10):105005. [PubMed: 25291210]

22. Diaz PM, Jenkins SV, Alhallak K, Semeniak D, Griffin RJ, Dings RP, et al. Quantitative diffuse reflectance spectroscopy of short-term changes in tumor oxygenation after radiation in a matched model of radiation resistance. Biomed Opt Express. 201; 9(8):3794–804. [PubMed: 30338156]

23. Chin LC, Cook EK, Yohan D, Kim A, Niu C, Wilson BC, et al. Early biomarker for radiation-induced wounds: day one postirradiation assessment using hemoglobin concentration measured from diffuse optical reflectance spectroscopy. Biomed Opt Express. 2017; 8(3):1682–8. [PubMed: 28663856]

24. Yu YH, Zhu X, Mo QG, Cui Y. Prediction of neoadjuvant chemotherapy response using diffuse optical spectroscopy in breast cancer. Clin Transl Oncol. 2018; 20(4):524–33. [PubMed: 28921461]

25. Troncoso JR, Diaz PM, Lee DE, Quick CM, Rajaram N. Longitudinal monitoring of tumor response to immune checkpoint inhibitors using noninvasive diffuse reflectance spectroscopy. Biomed Opt Express. 2021; 12(7):3982–91. [PubMed: 34457393]

26. Dadgar S, Troncoso JR, Siegel ER, Curry NM, Griffin RJ, Dings RP, et al. Spectroscopic investigation of radiation-induced reoxygenation in radiation-resistant tumors. Neoplasia. 2021; 23(1):49–57. [PubMed: 33220616]

27. Mundo AI, Greening GJ, Fahr MJ, Hale LN, Bullard EA, Rajaram N, et al. Diffuse reflectance spectroscopy to monitor murine colorectal tumor progression and therapeutic response. J Biomed Opt. 2020; 25(3):1–16.

28. Dadgar S, Troncoso JR, Rajaram N. Optical spectroscopic sensing of tumor hypoxia. J Biomed Opt. 2018; 23(6):1–6.

29. Rajaram N, Nguyen T, Tunnell JW. Lookup table-based inverse model for determining optical properties of turbid media. J Biomed Opt. 2008; 13(5):050501. [PubMed: 19021373]

30. Prahl S. Assorted Spectra [Internet]. 2018. Available from: https://www.omlc.org/spectra/.

31. Vishwanath K, Klein DH, Chang K, Schroeder T, Dewhirst MW, Ramanujam N. Quantitative optical spectroscopy can identify long-term local tumor control in irradiated murine head and neck xenografts. J Biomed Opt. 2009; 14(5):054051. [PubMed: 19895152]

32. Sunar U, Quon H, Durduran T, Zhang J, Du J, Zhou C, et al. Noninvasive diffuse optical measurement of blood flow and blood oxygenation for monitoring radiation therapy in patients with head and neck tumors: a pilot study. J Biomed Opt. 2006 Nov-Dec; 11(6):064021. [PubMed: 17212544]

33. Arnold KM, Flynn NJ, Raben A, Romak L, Yu Y, Dicker AP, et al. The impact of radiation on the tumor microenvironment: effect of dose and fractionation schedules. Cancer Growth Metastasis. 2018; 11:1179064418761639.

34. Jarosz-Biej M, Smolarczyk R, Cicho T, Kułach N. Tumor microenvironment as a "game changer" in cancer radiotherapy. Int J Mol Sci. 2019; 20(13):3212. [PubMed: 31261963]

35. Abdlaty R, Doerwald-Munoz L, Farrell TJ, Hayward JE, Fang Q. Hyperspectral imaging assessment for radiotherapy induced skin-erythema: Pilot study. Photodiagnosis Photodyn Ther. 2021; 33:102195. [PubMed: 33515761]

36. Hockel M, Vaupel P. Tumor hypoxia: definitions and current clinical, biologic, and molecular aspects. J Natl Cancer Inst. 2001; 93(4):266–76. [PubMed: 11181773]

37. Palmer GM, Viola RJ, Schroeder T, Yarmolenko PS, Dewhirst MW, Ramanujam N. Quantitative diffuse reflectance and fluorescence spectroscopy: tool to monitor tumor physiology in vivo. J Biomed Opt. 2009; 14(2):024010. [PubMed: 19405740]

38. Vala IS, Martins LR, Imaizumi N, Nunes RJ, Rino J, Kuonen F, et al. Low doses of ionizing radiation promote tumor growth and metastasis by enhancing angiogenesis. PloS One. 2010; 5(6):e11222. [PubMed: 20574535]

39. Chung SH, Feldman MD, Martinez D, Kim H, Putt ME, Busch DR, et al. Macroscopic optical physiological parameters correlate with microscopic proliferation and vessel area breast cancer signatures. Breast Cancer Res. 2015; 17(1):1–14. [PubMed: 25567532]

40. Cohen–Jonathan E, Bernhard EJ, McKenna WG. How does radiation kill cells? Curr Opin Chem Biol. 1999; 3(1):77–83. [PubMed: 10021401]

41. Najafi M, Motevaseli E, Shirazi A, Geraily G, Rezaeyan A, Norouzi F, et al. Mechanisms of inflammatory responses to radiation and normal tissues toxicity: clinical implications. Int J Radiat Biol. 2018; 94(4):335–56. [PubMed: 29504497]

42. Baselet B, Sonveaux P, Baatout S, Aerts A. Pathological effects of ionizing radiation: endothelial activation and dysfunction. Cellular Mol Life Sci. 2019; 76(4):699–728. [PubMed: 30377700]

43. Mourant JR, Freyer JP, Hielscher AH, Eick AA, Shen D, Johnson TM. Mechanisms of light scattering from biological cells relevant to noninvasive optical-tissue diagnostics. Applied Opt. 1998; 37(16):3586–93.

44. Vishwanath K, Yuan H, Barry WT, Dewhirst MW, Ramanujam N. Using optical spectroscopy to longitudinally monitor physiological changes within solid tumors. Neoplasia. 2009; 11(9):889–900. [PubMed: 19724683]

45. Tabassum S, Tank A, Wang F, Karrobi K, Vergato C, Bigio IJ, et al. Optical scattering as an early marker of apoptosis during chemotherapy and antiangiogenic therapy in murine models of prostate and breast cancer. Neoplasia. 2021; 23(3):294–303. [PubMed: 33578267]

46. Farhat G, Giles A, Kolios MC, Czarnota GJ. Optical coherence tomography spectral analysis for detecting apoptosis in vitro and in vivo. J Biomed Opt. 2015; 20(12):126001. [PubMed: 26641199]
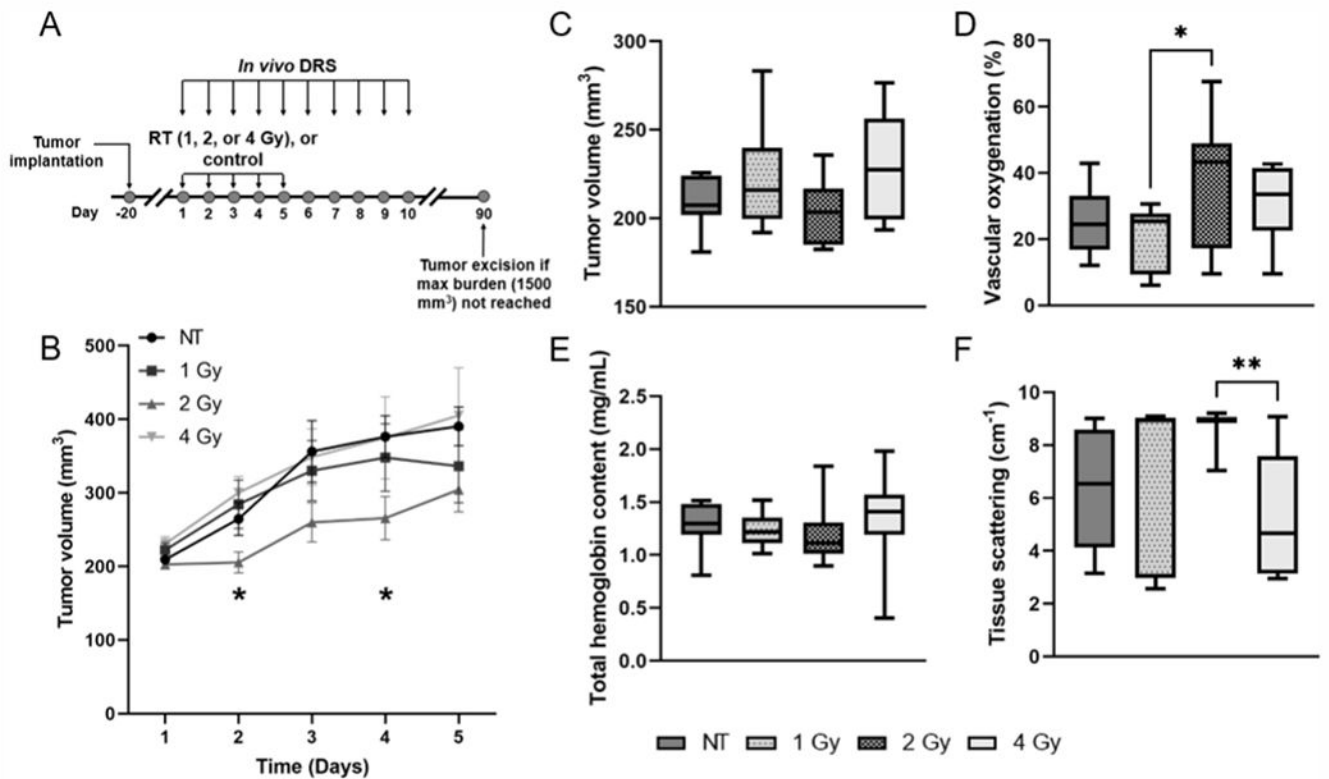
FIG. 1.

Panel A: Study design showing days of radiation treatment (RT) and optical measurements. Panel B: Average tumor volume measurements ± standard error of the mean (SEM) for each treatment group on the five days of treatment. *Represents significant differences in tumor volume between the 2 Gy/fraction and 4 Gy/fraction groups on day 2, and between the control (NT) and 2 Gy/fraction groups on day 4 of irradiation. Baseline comparison of (panel C) tumor volume, (panel D) vascular oxygenation, (panel E) total hemoglobin content and (panel F) tissue scattering between treatment groups. $*P < 0.05$ and $**P < 0.01$.
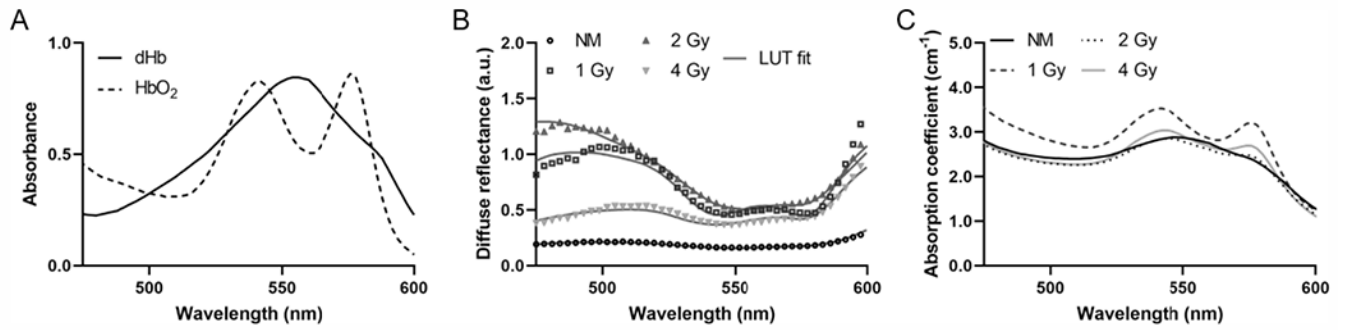
FIG. 2.
Panel A: Absorbance spectra of oxygenated and deoxygenated hemoglobin. Panel B: Representative diffuse reflectance spectra and their corresponding LUT fits from each group on day 3 of treatment. Panel C: Corresponding absorption spectra extracted from the LUT fits.
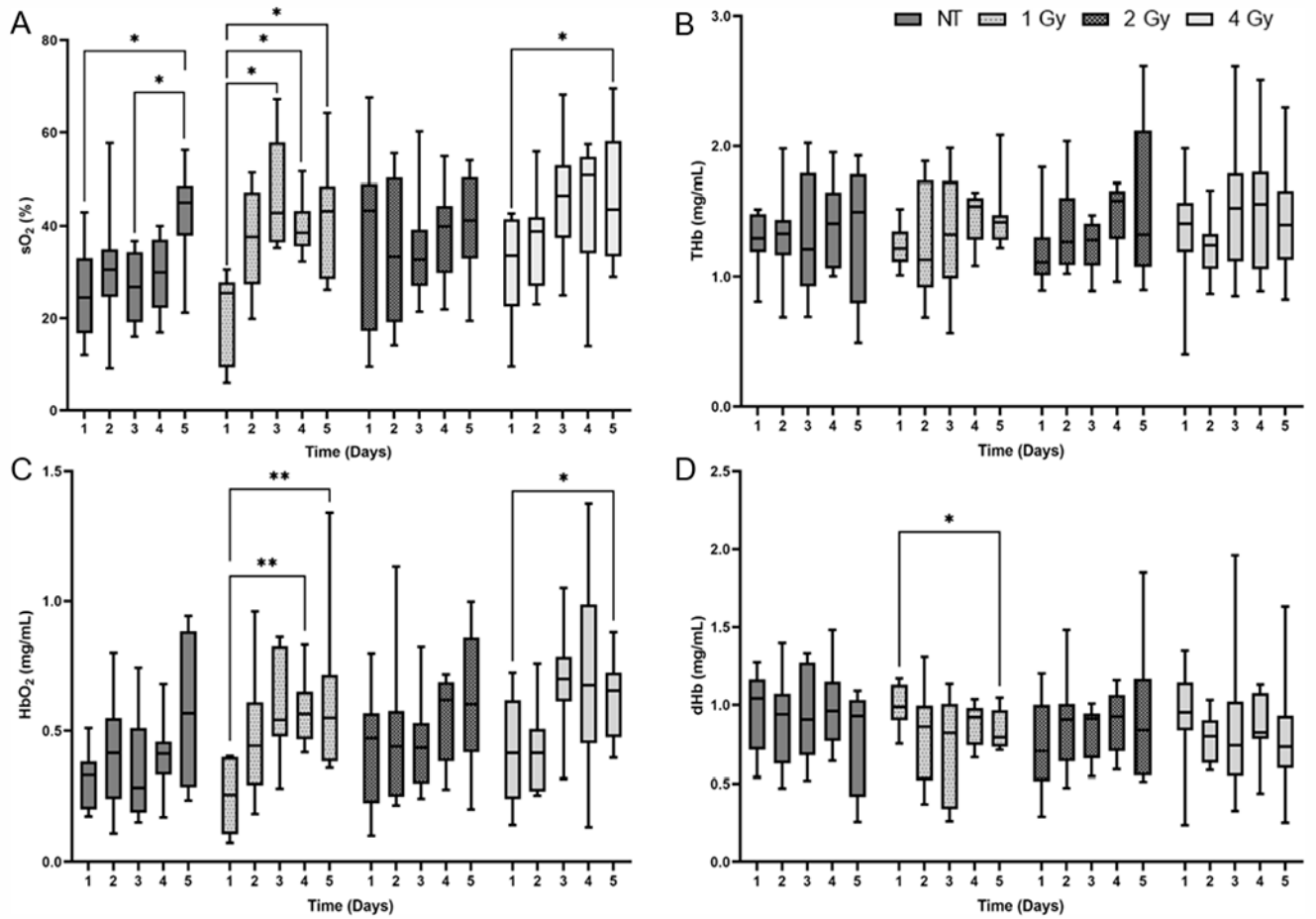
FIG. 3.
Changes in (panel A) vascular oxygenation, (panel B) total-hemoglobin concentration, (panel C) oxygenated hemoglobin, and (panel D) deoxygenated hemoglobin prior to irradiation for each treatment group. Data shown as minimum to maximum values for each treatment group on each day. Significant differences between days within a group are represented using asterisks (*). *P < 0.05 and **P < 0.01.
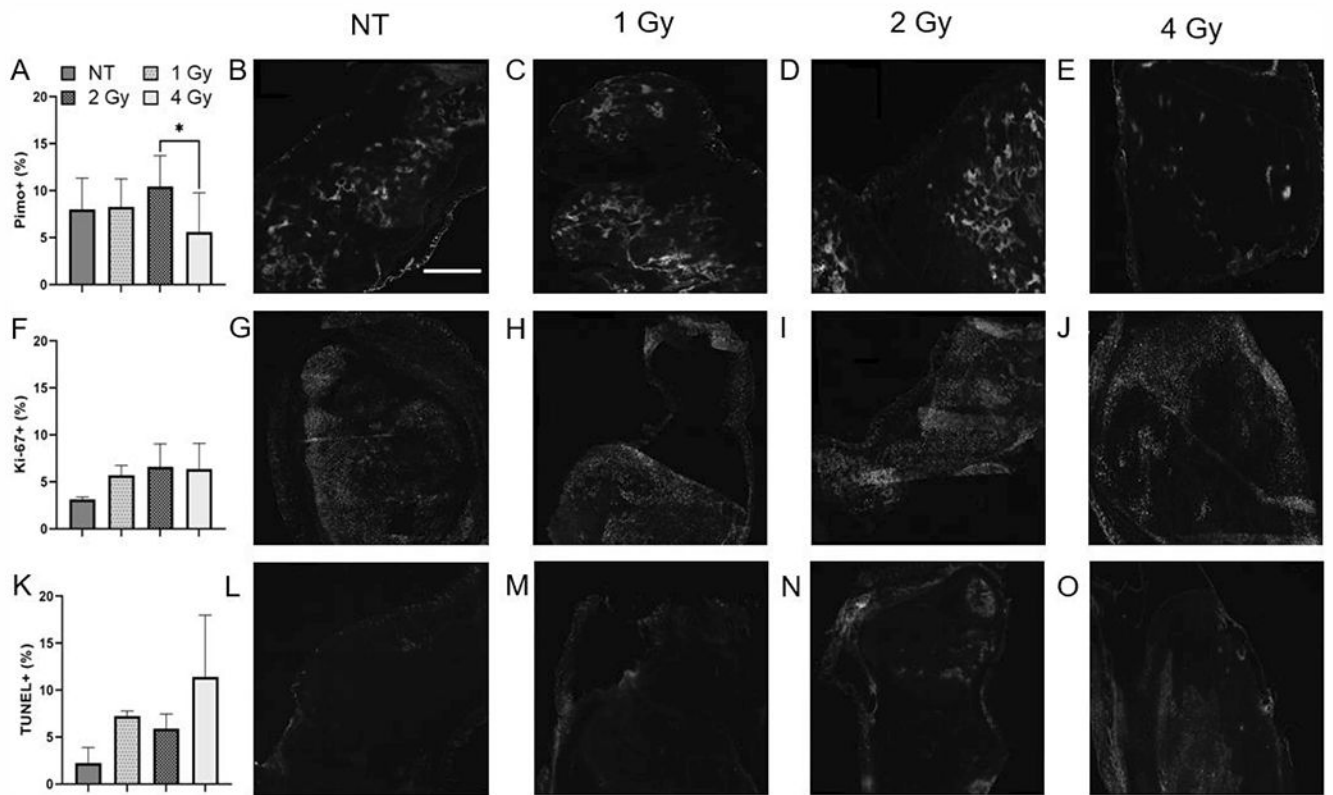
FIG. 4.
Quantification of (panel A) pimonidazole positive, (panel F) Ki-67 positive, and (panel K) TUNEL positive pixels in irradiated and non-irradiated tumors after five days of treatment. Representative images of (panels B–E) pimonidazole, (panels G–J) Ki-67 and (panels L–O) TUNEL stained slides. The scale bar represents 250 μm. *P < 0.05.
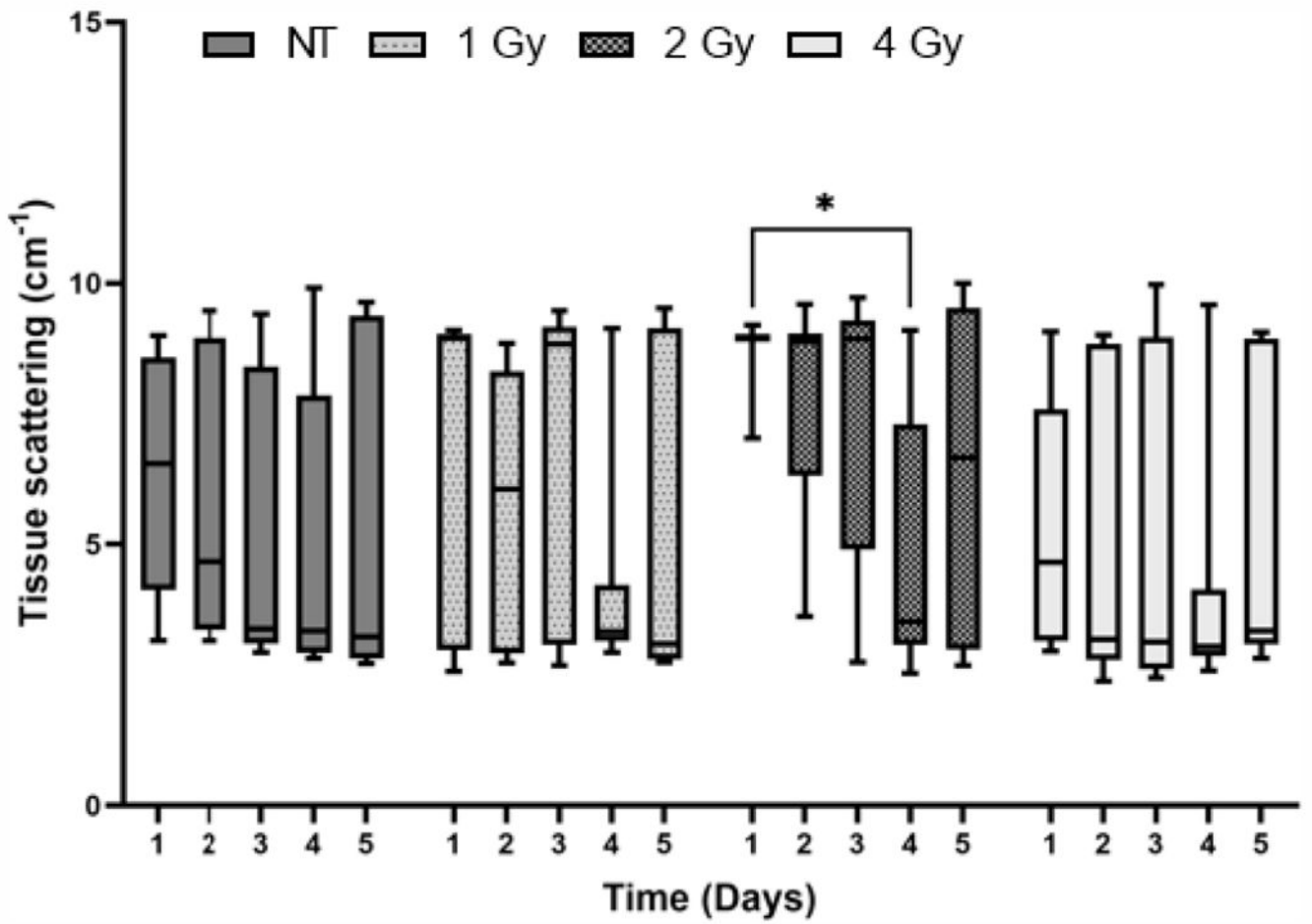
FIG. 5.
Tissue scattering before irradiation for each group on the five days of treatment. *P < 0.05.